

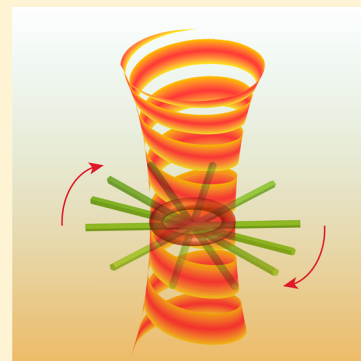
Optical Vortex Induced Rotation of Silver Nanowires

Zijie Yan and Norbert F. Scherer*

James Franck Institute and Department of Chemistry, The University of Chicago, 929 East 57th Street, Chicago, Illinois 60637, United States

S Supporting Information

ABSTRACT: Optical manipulation of metal nanowires offers the possibility to control the position, orientation, and associated motions of individual nanowires, particularly by utilizing their plasmonic properties. Here, we demonstrate that the orbital angular momentum of photons in Laguerre–Gauss (optical vortex) beams can induce rotation of single silver (Ag) nanowires with lengths of over 10 μm that are lying on (in molecular proximity to) a dielectric surface. We show that the rotation dynamics are governed by plasmonic interactions of the Ag nanowires with linearly polarized light, which yield a sinusoidal optical torque that causes angular acceleration. These results provide important information to understand the angular dependence of plasmonic nanowire–light interactions and extend the repertoire to realize applications in plasmonic lab-on-a-chip systems.

**SECTION:** Plasmonics, Optical Materials, and Hard Matter

Ag nanowires are plasmonic nanostructures that permit nanoscale confinement of light and transport of surface plasmons on the 10 μm scale.^{1–5} The ability to manipulate Ag nanowires by controlling the translation, alignment, and rotation of individual nanowires on substrate surfaces is important for utilizing nanowires as active components in nanophotonic devices and lab-on-a-chip systems.^{3,6} In particular, nanowires with controlled rotation could serve as nanomotors or mixers working in a liquid.⁷ However, the rotational motion of nanowires in fluids and especially those with polymer layers at surfaces, for example, polyvinylpyrrolidone (PVP) coating for Ag, is inhibited by strong viscous drag forces.⁸ Therefore, torques derived from external fields must be exerted on the nanowires to overcome the fluid drag. The driving fields and torques can be obtained from vector potentials such as rotating magnetic^{7,9} or electric fields.^{8,10} In fact, these have been used to rotate gold,^{8,10} platinum,⁸ and nickel^{7–9} nanowires in bulk solution.

Optical fields provide another, and very versatile, approach for orientational manipulation of elongated nanostructures, such as nanorods,^{11,12} bipyramids,¹³ and nanowires;^{14–18} these anisotropic particles can be fixed in space (or rotated) by a (rotating) linearly polarized optical beam. It is well-known that optical fields are able to rotate or spin objects.¹⁹ Rotation was demonstrated for special micro/nano-objects^{20,21} or optical fields²² with well-designed structures. However, rotation of a material could also be derived from photons and electromagnetic fields that carry spin and orbital angular momentum, which can be transferred to polarizable objects.^{23,24} Spin angular momentum arises from the spin of individual photons; each photon has an angular momentum of $\sigma_z \hbar$, where σ_z is ± 1 for circularly polarized light and 0 for linearly polarized light.²³

The photon spin angular momentum associated with circular polarization was initially shown to rotate a birefringent waveplate¹⁹ and, more recently, single Ag nanowires and gold nanoparticles on a surface.^{17,25}

The orbital angular momentum of photons was first demonstrated by Allen et al.²⁶ This angular momentum is associated with the spatial distribution of the electromagnetic fields; the Laguerre–Gauss (i.e., vortex) beam is a typical example.^{26,27} An optical vortex is an optical beam with a phase structure of $e^{il\theta}$, where l is the azimuthal mode index, also known as the topological charge, and θ is the polar angle around the beam's propagation axis.^{27,28} The optical vortex can thus be thought of as a twisted beam with l intertwined helical phase fronts.²⁴ Unlike circularly polarized light, an optical vortex beam carries an orbital angular momentum of $l\hbar$ per photon and thus offers two ways to control the magnitude of the torque on an object, by varying the topological charge and/or the optical power. Optical vortices have been applied to trap and rotate micro- and nanoparticles^{23,27,29–31} and also semiconductor nanowires.^{15,32}

Because plasmonics can involve strong light–matter interactions, optical methods provide the possibility to exert large forces and torques on metal nanowires. However, to our knowledge, there has been no report showing that plasmonic nanowires can be rotated by the photon orbital angular momentum. In this Letter, we demonstrate that linearly polarized optical vortices can rotate single silver nanowires solely by the orbital angular momentum. More importantly, we

Received: July 3, 2013

Accepted: August 13, 2013

Published: August 13, 2013



show that the rotation dynamics are not only governed by the competition between the driven torque from the external field (i.e., orbital angular momentum of the optical vortex) and the fluid drag torque, which is true for the case of magnetic and electric field induced rotation,^{7–10} but are also regulated (and even determined) by plasmonic interactions of the nanowires with light.

We produced vortex beams by modulating the wavefront of a linearly polarized Gaussian beam (wavelength of 800 nm) with a spatial light modulator (SLM). The topological charge of a vortex beam can be easily changed by varying the phase modulation. The vortex beam was focused onto single Ag nanowires from the bottom side of a sample cell, as illustrated in Figure 1a; the sample cell consists of two coverslips separated by an annular adhesive spacer and is mounted on an inverted microscope.

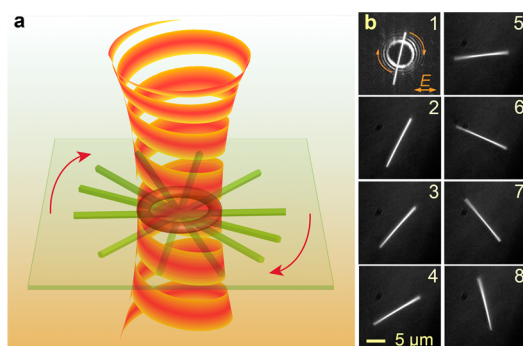


Figure 1. (a) Illustration of an optical vortex induced rotation of a single Ag nanowire lying on a glass surface. (b) Dark-field optical images of a Ag nanowire rotated by an optical vortex ($l = 20$). Snapshots (b2–8) were taken every 1/15 s with the scattered light from the vortex beam being blocked, while the first one (b1) is a composite image of the nanowire and the vortex.

Figure 1b demonstrates the optical vortex induced rotation of a single 14 μm long silver nanowire. An image of the optical vortex with a topological charge of $l = 20$ can be seen in panel b1 (recorded by removing the short-pass filter and collecting the scattered (reflected) light from the glass–water interface). The polarization of the beam was horizontal in the image. The Ag nanowire was rotating clockwise in a continuous manner, as shown in Figure 2a. The rotation was caused by the transfer of orbital angular momentum from the optical vortex to the nanowire. Although the orbital angular momentum has no angular dependence,²⁶ we found that the rotation speed of the nanowire was not uniform, as is clearly seen in Figure 2b. This polar plot shows that the angular velocity of the nanowire depends strongly on its long-axis direction. Moreover, the polar plot exhibits a dipole-like pattern. The rotation slowed down when the wire was oriented nearly vertical and accelerated when it was horizontal, indicating that the polarization of the vortex beam plays a role. It is known that Ag nanowires tend to align perpendicular to the polarization direction of a linearly polarized light.^{16,17} The perpendicular orientation is due to the unique plasmonic interaction-induced torque on Ag nanowires,¹⁶ and this tendency creates a potential minimum around that perpendicular direction and a barrier to Ag nanowire rotation.

Because the rotation is induced by the transfer of orbital angular momentum, changing the sign of the topological charge of the vortex should reverse the rotation direction. This effect is

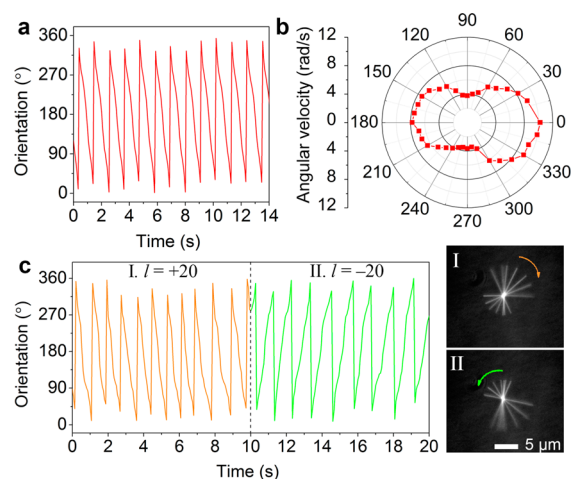


Figure 2. (a) Time trajectory of the nanowire orientations. (b) Polar plot of the angular velocity of the nanowire. The velocity is in the radial coordinate, while the angle is in the lab frame. (c) Time trajectory of the orientations of another nanowire (see Video 1 (jz401381e_si_001.avi), Supporting Information). At 10 s, the topological charge of the vortex was changed from 20 to -20 . As a result, the nanowire changed its rotation direction, as shown in the images on the right; each image is a superposition of frames taken over a 0.5 s window.

demonstrated in Figure 2c, where after changing the topological charge from $+20$ to -20 (by altering the phase mask on the SLM), a nanowire ($\sim 11 \mu\text{m}$ long) reversed its rotation direction from clockwise to counterclockwise. This nanowire, as well as all of the others (more than 10) that we have studied, showed similar nonuniform rotation behaviors.

The vortices could not exert detectable attractive (nor repulsive) force to translate the nanowires near the bottom coverslip surface, that is, if we move the vortex away from the wires (equivalently, by shifting the coverslip and the wires with a piezo-stage), the wires will stay at the same position instead of moving with the vortex; an example is shown in Video 2 (jz401381e_si_002.avi, Supporting Information). Because the vortices cannot trap Ag nanowires, the rotation axis of a nanowire depends on the positions illuminated by the vortex beam. The asymmetry of the curve in Figure 2b (i.e., deviation between 0 and 180°) is due to the fact that the center of the vortex beam was not at the midpoint of the nanowire. The observed asymmetry in the angular velocity can result from an asymmetry in the optical beam³³ or from an asymmetry in the frictional drag. We used a Shack–Hartmann wavefront sensor and determined that the beam is quite symmetric (also note the result in Figure 4). Therefore, we attribute the asymmetry in velocity to details of the Ag nanowire (and PVP coating) interaction with the coverslip surface, that is, a surface inhomogeneity.

It is worth noting that the coverslip must exert some attractive forces (i.e., a van der Waals force or electrostatic force) on the Ag nanowires; otherwise, they would be pushed away by the (repulsive) scattering forces from the vortex beam (as we observed for nanowires in the solution). A balance of the attractive and repulsive forces determines the separation between the nanowire and the substrate surface. Because the scattering force will change when the topological charge is varied, the position of the nanowire relative to the focal plane of the vortex beam (coincident with the glass surface) will change slightly. This change will affect the driven torque that depends

on the optical intensity and thus influences the rotation dynamics of the nanowire. On the other hand, if the attractive force is too strong, the nanowires will be stuck on the surface and cannot be rotated. Nevertheless, a partially stuck nanowire may provide extra rotation modalities. Video 3 (jz401381e_si_003.avi, Supporting Information) shows that when one end of a Ag nanowire was stuck on the surface, we could use the vortex beams to rotate the other end in three dimensions with a cone-shape trajectory. There the topological charge controlled both wire rotation (precession) and angle of projection along the surface normal.

To further reveal the rotation dynamics, we focused the vortex beam on a Ag nanowire ($\sim 13.6 \mu\text{m}$ long) and then changed the topological charges to generate a series of optical vortices. Moreover, we carefully positioned the nanowire by moving the coverslip with a piezo-stage so that the center of the beam was coincident with the midpoint of the wire. Figure 3a

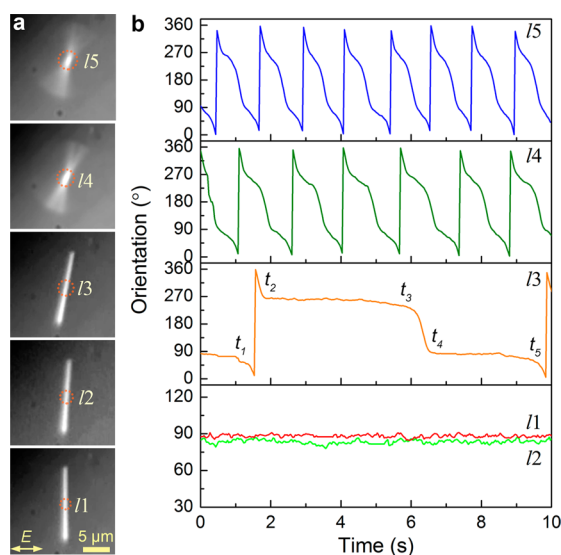


Figure 3. (a) Optical images of a Ag nanowire rotated by optical vortices (indicated by the dashed circles) with different topological charges (see Video 4 (jz401381e_si_004.avi), Supporting Information). The first two images are superpositions of frames taken in 1 s with a frame rate of 30 fps, and the rest are representative images in each case. (b) Time trajectories of the wire orientations with different topological charges.

shows the optical images of the nanowire interacting with optical vortices of $l = 5$ to 1, and Figure 3b shows the time trajectories of the motions. When $l = 5$ and 4, the nanowire could be rotated continuously, but the time T_1 required to rotate 360° was longer for $l = 4$ ($T_4 = 1.6$ s versus $T_5 = 1.2$ s). When $l = 3$, the nanowire could be still be rotated but tended to get stuck at a certain orientation (θ_1) for a long time, for example, at $\sim 261^\circ$ (i.e., 81°) from t_2 to t_3 and at $\sim 81^\circ$ from t_4 to t_5 . When $l = 2$ and 1, the same nanowire could not be rotated anymore but became stuck at $\theta_2 = 84^\circ$ and $\theta_1 = 87^\circ$, respectively. The angular velocities of the nanowire motion have a clear dipole-like angular dependence for $l = 5$ to 3, as shown in Figure 4, and the velocity at a given angle is greater for larger l . The angular velocity, ω , can be fitted with a function $\omega(\theta) = a + b \sin[2(\theta + c)]$ with the parameters shown in Table 1. Because the orbital angular force is uniform, the dipolar velocity pattern indicates that a sinusoidal hindrance (or cosinusoidal driving force) is exerted on the nanowire.

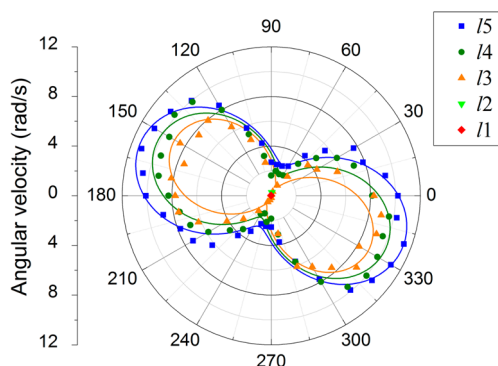


Figure 4. Polar plot of the angular velocities of the nanowire rotated by optical vortices with different topological charges (analyzed from the data shown in Figure 3b). The direction of the linear polarization is 90° . The solids curves are sinusoidal fittings of the data with the function and parameters shown in Table 1.

Table 1. Parameters of the Angular Velocity Curves in Figure 4 Fit with $\omega(\theta) = a + b \sin[2(\theta + c)]$

l	a	b	c (deg)
5	7.03	4.33	66
4	6.03	4.12	70
3	4.86	4.07	75

Consider a Ag nanowire interacting with an optical vortex, as illustrated in Figure 5a; the vortex beam will exert an optical force, F_l , on the nanowire due to the transfer of orbital angular momentum. The polarization effect also exerts an optical force, F_E , on the nanowire due to plasmonic interactions. We assume that the positive direction of this force is in the counter-clockwise direction. Finally, the fluid (and frictional interaction with the surface) will exert a viscous drag force, F_d , on the nanowire with a direction always opposite to the rotation direction.⁸ Because the laser power of an optical vortex is distributed around a ring or annulus and there was no observable thermal effect on the nanowires, here, we neglect the influence from the substrate and force related to thermal fluctuations that otherwise result in Brownian motion.³⁴ The forces F_l , F_E , and F_d will yield torques of τ_l , τ_E , and τ_d , respectively, on the nanowire with the net torque

$$\tau_{\text{net}} = \tau_l - \tau_E - \tau_d \quad (1)$$

The torque from the orbital angular momentum is proportional to the transferred photon angular momentum,^{27,34} that is, proportional to the light intensity (I_l) times the absorption cross section obtained from the FDTD simulation of the nanowire (σ_{abs}). The vortex contains a bright ring with a radius of R_l and a width comparable to λ ,²⁷ which is the wavelength of light in the liquid medium. For small values of l , $R_l = a\sqrt{l}$, where a is a constant.³⁵ The radii of our vortices measured from the optical images are also consistent with this relationship. Assuming that the power of the incident beam, P , is spread uniformly around the bright ring, then the light intensity is²⁷

$$I_l \approx \frac{P}{2\pi\lambda R_l} = \frac{P}{2\pi\lambda a\sqrt{l}} \quad (2)$$

Because each photon carries a momentum of $\hbar l$, the torque from the photon orbital angular momentum is²³

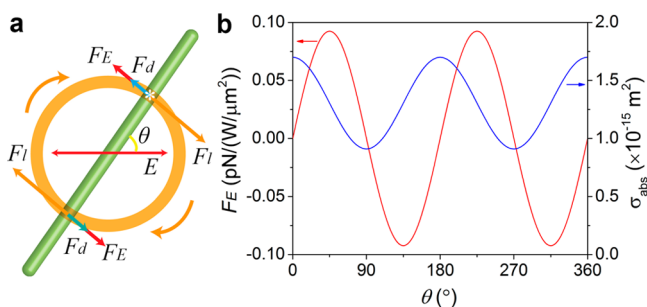


Figure 5. (a) Schematic of the forces on a Ag nanowire rotated by a linearly polarized optical vortex. The center of the vortex is coincident with the midpoint of the wire. The angle between the long axis of the wire and the polarization direction of the light is θ (the same as the convention of Figures 2–4). F_l , F_E , and F_d denote the forces from the photon orbital angular momentum, the plasmonic interactions, and the fluid drag, respectively. (b) Angular dependence of the force F_E on one illuminated portion of a Ag nanowire (i.e., the portion marked by a * in panel a) and the absorption cross section σ_{abs} obtained by FDTD simulations. The Ag nanowire is approximated as a 10 μm long cylinder capped with hemispherical ends with diameters of 80 nm, and the illuminated portion is 0.6 μm long and 3 μm away from the midpoint of the nanowire.

$$\tau_l = \frac{I_l \sigma_{\text{abs}} \hbar l}{\hbar \omega_0} \approx \frac{P \sigma_{\text{abs}} \sqrt{l}}{2\pi \lambda a \omega_0} \quad (3)$$

where ω_0 is the frequency of the light. Because the Ag nanowire was rotated slowly, the fluid could be considered in the Stokes flow region (linear response), and the fluid drag torque on a nanowire can be expressed as⁹

$$\tau_d \approx \frac{\pi}{3} J \eta L^3 \omega \quad (4)$$

where η is the dynamic viscosity of the fluid, L is the length of the nanowire, and J is approximately a constant.

We performed three-dimensional finite-difference time-domain (FDTD) simulations to determine the angular dependence of the optical force F_E exerted on one illuminated portion (marked by an asterisk) of a nanowire, as illustrated in Figure 5a (the force on the other portion has the same amplitude but the opposite direction), and the absorption cross section. The calculated results are shown in Figure 5b. The force curve follows a function of $F_E(\theta) = M \sin(2\theta)$,³³ where M depends on the wire sizes but is a constant for a certain nanowire in units of $\text{pN}/(\text{W}/\mu\text{m}^2)$. This is just a sinusoidal driven force required to generate the dipole-like angular velocity curves in Figure 4. The absorption cross section follows a function of $\sigma_{\text{abs}}(\theta) = m + n \sin(2\theta + 90^\circ)$, where $m = 1.3 \times 10^{-15} \text{ m}^2$ and $n = 0.4 \times 10^{-15} \text{ m}^2$. Note that the calculated optical force is normalized to the light intensity. In the case of an annular beam, the total torque arm is R_l , and the torque is

$$\tau_E = I_l M \sin(2\theta) R_l = \frac{PM \sin(2\theta)}{2\pi \lambda} \quad (5)$$

Substituting eqs 3–5 into eq 1, we get

$$\tau_{\text{net}} \approx \frac{P \sigma_{\text{abs}} \sqrt{l}}{2\pi \lambda a \omega_0} - \frac{\pi}{3} J \eta L^3 \omega - \frac{PM \sin(2\theta)}{2\pi \lambda} \quad (6)$$

Note that

$$\tau_{\text{net}} = I \frac{d\omega}{dt} \quad (7)$$

where I is the momentum of inertia of the nanowire in the liquid (by which we also mean this to include the frictional interaction with the surface); therefore, we finally get the equation of motion of the nanowire

$$A \sqrt{l} [m + n \sin(2\theta + 90^\circ)] - B\omega - C \sin(2\theta) \approx I \frac{d\omega}{dt} \quad (8)$$

where A , B , and C are approximately constants for a certain nanowire. This equation shows that as the topological charge decreases, the torque τ_l will decrease, while the maximum value of the torque τ_E stays the same. This explains why the nanowire shown in Figure 3 could be rotated by optical vortices of $l = 5$ and 4, but was partially stuck at $l = 3$ and finally stopped rotating at $l = 2$ and 1. Similarly, the greater angular velocity at larger l can be understood due to the larger torque generated by the orbital angular momentum. Because τ_E increases from $\theta = 90^\circ$ to 45° (see Figure 5b), a larger torque of τ_l also means that the critical angle, where the nanowire tends to be stuck, would be closer to 45° at larger l . Again, this is consistent with the experimental results. Since the contributions to the torque in eqs 3 and 5 have angular dependence (shown in Figure 5b) but they are shifted by 90° , the maximum angular velocity does not occur at $\theta = 0^\circ$ or 90° . In the limit that the contribution from eq 3 is much larger, the dipolar velocity profile should be aligned along the 0° – 180° axis; this is the case shown in Figure 2b for $l = 20$. Finally, some factors could affect the quantitative accuracy of the predictions, such as the influence of the substrate and the (weak) angular dependence of the absorption cross section, as discussed above.

We have demonstrated that the transfer of orbital angular momentum from a linearly polarized optical vortex to a Ag nanowire can induce rotation of the wire in liquid. The rotation is a competition between the driven torque from the photon orbital angular momentum and “damping” torques, including the fluid drag torque and optical torque arising from plasmonic interactions of the nanowire with the optical field. The competition results in nonuniform rotation of single silver nanowires with apparent acceleration, which can be well explained by an intuitively reasonable equation of motion. Moreover, translation of Ag nanowires can be accomplished by other optical beam profiles, such as Bessel beams.^{16,18} Therefore, by simply changing the phase mask on the SLM to modulate the same incident Gaussian beam into another structured beam, one could translate (position) and rotate (orient) metallic nanowires near transparent dielectric surfaces. This optical rotation method may have potential application in plasmonic lab-on-a-chip systems, where the plasmonic nanowires could serve as fluid-stirring bars while providing optical field enhancement for sensing and biomedical diagnostics and even for heating for localized chemical reactions.

METHODS

The Laguerre–Gauss (optical vortex) beams were generated by wavefront modulation of a linearly polarized Gaussian beam from a cw-Ti:Sapphire laser (wavelength of 800 nm, power of 100 mW).¹⁸ A SLM (Hamamatsu X10468) was used to perform the phase modulation with designed phase masks (holograms) to generate different topological charges. Basically, the SLM creates a vortex beam profile of $E(r) = u(r)e^{il\theta}$ from an incident Gaussian beam, where r denotes the radial coordinate and $u(r)$ is the amplitude of the Gaussian beam. The phase-modulated (i.e., vortex) beam was relayed by two lenses and

focused by a 60 \times water immersion objective (NA 1.2, Olympus UPLSAPO) onto the bottom coverslip of a sample cell that consists of two coverslips (Fisherbrand cover glasses #12-541B; cleaned with Milli-Q water) separated by an annular adhesive spacer. The sample cell was filled with an aqueous solution of Ag nanowires. The nanowires were imaged by dark-field microscopy using an inverted microscope (Olympus IX71). The backscattered light of the vortex beam was attenuated by a short-pass filter to ensure clear (low background) imaging of the nanowires. Image analysis of the wire motions was performed by customized codes written in MATLAB. The angular velocity of a rotating nanowire is approximated as the mean angular velocity at the mean orientation (angle) of the nanowire between two consecutive frames (generally the change of orientation is <10 $^\circ$).

The silver nanowires were synthesized following a well-established polyol process,^{36,37} and they were \sim 80 nm in diameter and over 10 μ m in length with a surface coating of PVP. Due to their density and specific gravity, the nanowires quickly settled to the bottom coverslip. However, the wires did not become irreversibly bound to the surface by van der Waals forces for about 0.5 hour. We could manipulate individual Ag nanowires during this 30 min window, which could presumably be extended by suitable surface treatment of the coverslip. In fact, we have done control experiments using UV/ozone-treated coverslips that are negatively charged. In this case, the nanowires could remain suspended in the sample cell for hours; although most of them settle to the bottom of the sample cell after \sim 0.5 h, they do not become irreversibly bound to the coverslip. However, in this case, the nanowires would be easily pushed away by the scattering force from the vortex beams. Therefore, in order to controllably rotate the nanowires, we need some attractive forces to confine the nanowires near the substrate.

Three-dimensional FDTD simulations were performed using the commercial software package FDTD Solutions (Lumerical, Inc.). The nanowire is approximated as a Ag cylinder (diameter of 80 nm and length of 10 μ m) capped with hemispherical ends (diameter of 80 nm). The refractive index of Ag is set as $n = 0.04 + i5.57$,³⁸ and that of the environment is set as 1.33 (i.e., water). A portion of the Ag nanowire, which is 0.6 μ m long and 3 μ m away from the midpoint, is illuminated by a linear polarized plane wave with a wavelength of 800 nm. The nanowire lies in the x - y plane while the wave propagates in the z -direction. The simulation region is $0.4 \times 0.4 \times 0.8 \mu\text{m}^3$. A nonuniform mesh is used with a maximum grid size of 4 nm in a $0.15 \times 0.15 \times 0.6 \mu\text{m}^3$ region enclosing the illuminated portion of the nanowire. The time step for simulation is 0.0095 fs. Optical forces on the nanowire were calculated by integrating the Maxwell stress tensor over a surface surrounding the illuminated portion of the nanowire. By changing the polarization direction, we can calculate the angular dependence of the optical force F_E exerted on the nanowire and the absorption cross section.

■ ASSOCIATED CONTENT

■ Supporting Information

Video clips showing the optical vortex induced rotation of Ag nanowires. This material is available free of charge via the Internet at <http://pubs.acs.org>.

■ AUTHOR INFORMATION

Corresponding Author

*E-mail: nfschere@uchicago.edu.

Notes

The authors declare no competing financial interest.

■ ACKNOWLEDGMENTS

This work was supported by the National Science Foundation CCI Program (CHE-0802913). We thank Dr. Julian Sweet for assistance with the setup of the optical system.

■ REFERENCES

- (1) Ditlbacher, H.; Hohenau, A.; Wagner, D.; Kreibig, U.; Rogers, M.; Hofer, F.; Aussenegg, F. R.; Krenn, J. R. Silver Nanowires as Surface Plasmon Resonators. *Phys. Rev. Lett.* **2005**, *95*, 257403.
- (2) Wild, B.; Cao, L.; Sun, Y.; Khanal, B. P.; Zubarev, E. R.; Gray, S. K.; Scherer, N. F.; Pelton, M. Propagation Lengths and Group Velocities of Plasmons in Chemically Synthesized Gold and Silver Nanowires. *ACS Nano* **2012**, *6*, 472–482.
- (3) Lal, S.; Link, S.; Halas, N. J. Nano-Optics from Sensing to Waveguiding. *Nat. Photon.* **2007**, *1*, 641–648.
- (4) Wei, H.; Zhang, S. P.; Tian, X. R.; Xu, H. X. Highly Tunable Propagating Surface Plasmons on Supported Silver Nanowires. *Proc. Natl. Acad. Sci. U.S.A.* **2013**, *110*, 4494–4499.
- (5) Liu, Z.; Ricks, A. M.; Wang, H.; Song, N.; Fan, F.; Zou, S.; Lian, T. High-Resolution Imaging of Electric Field Enhancement and Energy-Transfer Quenching by a Single Silver Nanowire Using QD-Modified AFM Tips. *J. Phys. Chem. Lett.* **2013**, 2284–2291.
- (6) Guo, X.; Ma, Y.; Wang, Y.; Tong, L. Nanowire Plasmonic Waveguides, Circuits and Devices. *Laser Photon. Rev.* **2013**, DOI: 10.1002/lpor.201200067.
- (7) Zhang, L.; Petit, T.; Lu, Y.; Kratochvil, B. E.; Peyer, K. E.; Pei, R.; Lou, J.; Nelson, B. J. Controlled Propulsion and Cargo Transport of Rotating Nickel Nanowires near a Patterned Solid Surface. *ACS Nano* **2010**, *4*, 6228–6234.
- (8) Fan, D. L.; Zhu, F. Q.; Cammarata, R. C.; Chien, C. L. Controllable High-Speed Rotation of Nanowires. *Phys. Rev. Lett.* **2005**, *94*, 247208.
- (9) Keshoju, K.; Xing, H.; Sun, L. Magnetic Field Driven Nanowire Rotation in Suspension. *Appl. Phys. Lett.* **2007**, *91*, 123114.
- (10) Edwards, B.; Mayer, T. S.; Bhiladvala, R. B. Synchronous Electrorotation of Nanowires In Fluid. *Nano Lett.* **2006**, *6*, 626–632.
- (11) Pelton, M.; Liu, M. Z.; Kim, H. Y.; Smith, G.; Guyot-Sionnest, P.; Scherer, N. E. Optical Trapping and Alignment of Single Gold Nanorods by Using Plasmon Resonances. *Opt. Lett.* **2006**, *31*, 2075–2077.
- (12) Ruijgrok, P. V.; Verhart, N. R.; Zijlstra, P.; Tchebotareva, A. L.; Orrit, M. Brownian Fluctuations and Heating of an Optically Aligned Gold Nanorod. *Phys. Rev. Lett.* **2011**, *107*, 037401.
- (13) Toussaint, K. C., Jr.; Liu, M.; Pelton, M.; Pesic, J.; Guffey, M. J.; Guyot-Sionnest, P.; Scherer, N. F. Plasmon Resonance-Based Optical Trapping of Single and Multiple Au Nanoparticles. *Opt. Express* **2007**, *15*, 12017–12029.
- (14) Pauzuskie, P. J.; Radenovic, A.; Trepagnier, E.; Shroff, H.; Yang, P. D.; Liphardt, J. Optical Trapping and Integration of Semiconductor Nanowire Assemblies in Water. *Nat. Mater.* **2006**, *5*, 97–101.
- (15) Agarwal, R.; Ladavac, K.; Roichman, Y.; Yu, G.; Lieber, C.; Grier, D. Manipulation and Assembly Of Nanowires with Holographic Optical Traps. *Opt. Express* **2005**, *13*, 8906–8912.
- (16) Yan, Z.; Sweet, J.; Jureller, J. E.; Guffey, M. J.; Pelton, M.; Scherer, N. F. Controlling the Position and Orientation of Single Silver Nanowires on a Surface Using Structured Optical Fields. *ACS Nano* **2012**, *6*, 8144–8155.
- (17) Tong, L.; Miljkovic, V. D.; Käll, M. Alignment, Rotation, and Spinning of Single Plasmonic Nanoparticles and Nanowires Using

Polarization Dependent Optical Forces. *Nano Lett.* **2010**, *10*, 268–273.

(18) Yan, Z.; Jureller, J. E.; Sweet, J.; Guffey, M. J.; Pelton, M.; Scherer, N. F. Three-Dimensional Optical Trapping and Manipulation of Single Silver Nanowires. *Nano Lett.* **2012**, *12*, 5155–5161.

(19) Beth, R. A. Mechanical Detection and Measurement of the Angular Momentum of Light. *Phys. Rev.* **1936**, *50*, 115–125.

(20) Galajda, P.; Ormos, P. Complex Micromachines Produced and Driven by Light. *Appl. Phys. Lett.* **2001**, *78*, 249–251.

(21) Liu, M.; Zentgraf, T.; Liu, Y.; Bartal, G.; Zhang, X. Light-Driven Nanoscale Plasmonic Motors. *Nat. Nanotechnol.* **2010**, *5*, 570–573.

(22) Paterson, L.; MacDonald, M. P.; Arlt, J.; Sibbett, W.; Bryant, P. E.; Dholakia, K. Controlled Rotation of Optically Trapped Microscopic Particles. *Science* **2001**, *292*, 912–914.

(23) Friese, M. E. J.; Enger, J.; Rubinsztein-Dunlop, H.; Heckenberg, N. R. Optical Angular-Momentum Transfer to Trapped Absorbing Particles. *Phys. Rev. A* **1996**, *54*, 1593–1596.

(24) Padgett, M.; Bowman, R. Tweezers with a Twist. *Nat. Photon.* **2011**, *5*, 343–348.

(25) Lehmuskero, A.; Ogier, R.; Gschneidner, T.; Johansson, P.; Käll, M. Ultrafast Spinning of Gold Nanoparticles in Water Using Circularly Polarized Light. *Nano Lett.* **2013**, *13*, 3129–3134.

(26) Allen, L.; Beijersbergen, M. W.; Spreeuw, R. J. C.; Woerdman, J. P. Orbital Angular Momentum of Light and the Transformation of Laguerre–Gaussian Laser Modes. *Phys. Rev. A* **1992**, *45*, 8185–8189.

(27) Curtis, J. E.; Grier, D. G. Structure of Optical Vortices. *Phys. Rev. Lett.* **2003**, *90*, 133901.

(28) Ng, J.; Lin, Z.; Chan, C. T. Theory of Optical Trapping by an Optical Vortex Beam. *Phys. Rev. Lett.* **2010**, *104*, 103601.

(29) Dienerowitz, M.; Mazilu, M.; Reece, P. J.; Krauss, T. F.; Dholakia, K. Optical Vortex Trap for Resonant Confinement of Metal Nanoparticles. *Opt. Express* **2008**, *16*, 4991–4999.

(30) Tao, S.; Yuan, X. C.; Lin, J.; Peng, X.; Niu, H. Fractional Optical Vortex Beam Induced Rotation of Particles. *Opt. Express* **2005**, *13*, 7726–7731.

(31) Ladavac, K.; Grier, D. G. Colloidal Hydrodynamic Coupling in Concentric Optical Vortices. *Europhys. Lett.* **2005**, *70*, 548–554.

(32) Shi, L.; Li, J.; Tao, T.; Wu, X. Rotation of Nanowires With Radially Higher-Order Laguerre–Gaussian Beams Produced by Computer-Generated Holograms. *Appl. Opt.* **2012**, *51*, 6398–6402.

(33) Simpson, S. H.; Hanna, S. Optical Angular Momentum Transfer by Laguerre–Gaussian Beams. *J. Opt. Soc. Am. A* **2009**, *26*, 625–638.

(34) O’Neil, A. T.; MacVicar, I.; Allen, L.; Padgett, M. J. Intrinsic and Extrinsic Nature of the Orbital Angular Momentum of a Light Beam. *Phys. Rev. Lett.* **2002**, *88*, 053601.

(35) Padgett, M. J.; Allen, L. The Poynting Vector in Laguerre–Gaussian Laser Modes. *Opt. Commun.* **1995**, *121*, 36–40.

(36) Sun, Y.; Gates, B.; Mayers, B.; Xia, Y. Crystalline Silver Nanowires by Soft Solution Processing. *Nano Lett.* **2002**, *2*, 165–168.

(37) Wiley, B.; Sun, Y.; Xia, Y. Polyol Synthesis of Silver Nanostructures: Control of Product Morphology with Fe(II) or Fe(III) Species. *Langmuir* **2005**, *21*, 8077–8080.

(38) Johnson, P. B.; Christy, R. W. Optical Constants of the Noble Metals. *Phys. Rev. B* **1972**, *6*, 4370–4379.